

# Experimental study on performance analysis of Oscillating Water Column Wave Energy Converter integrated into breakwater

Sewan Park, Kyong-Hwan Kim, Kwang Ho Lee, Jeong-Seok Kim, Bo-Woo Nam, Keyyong Hong

**Abstract**— Korea Research Institute of Ships and Ocean Engineering (KRISO) is developing an oscillating water column (OWC) wave energy converter through a government funded project to integrate the OWC into breakwaters for the purpose of supplying clean energy to the island area. In the previous study, a sloped OWC chamber that can be easily constructed on an existing conventional breakwater has been developed, and its performance for primary energy conversion has been evaluated by using various analysis methods. In this study, the performance of primary energy conversion for the sloped OWC chamber integrated into the breakwater was evaluated by the experimental method. The experiment was carried out in the shallow water wave basin with modelling the PTO (Power Take-Off) as an orifice and the breakwater as scaled tetrapods and base structures with a scale ratio of 1/20. The regular wave test for various incident wave period as well as various wave slopes was performed to measure the water surface level inside the chamber, the differential pressure between the inside of the chamber and the atmosphere, and the airflow speed through the orifice. By comparing results for various wave condition and with or without the presence of the breakwater, effect of the wave slope dependency and the presence of the breakwater on the OWC performance was discussed.

**Keywords**—Oscillating Water Column (OWC), Primary Energy Conversion, Wave Basin Model Tests, Breakwater Effects

Paper ID: WDD-1839

This research was supported by a grant from National R&D Project "Development of Wave Energy Converters Applicable to Breakwater and Connected Micro-Grid with Energy Storage System" funded by Ministry of Oceans and Fisheries, Korea (PMS4030) and by a grant from Endowment Project of "Development of WECAN for the Establishment of Integrated Performance and Structural Safety Analytical Tools of Wave Energy Converter" funded by Korea Research Institute of Ships and Ocean engineering (PES3240). All support is gratefully acknowledged.

S. Park, K.-H. Kim, J.-S. Kim, B.-W. Nam, and K. Hong is with Offshore Plant and Marine Energy Research Division in KRISO, 32, Yuseong-daero 1312beon-gil, Yuseong-gu, Daejeon, 34103 Korea (corresponding author's e-mail: [khong@kriso.re.kr](mailto:khong@kriso.re.kr)).

K. H. Lee is with Department of Energy Resources and Plant Engineering in Catholic Kwandong University, 24, Beomil-ro 579beon-gil, Gangneung-si, Gangwon-do, 25601 Korea (e-mail: [frong0215@gmail.com](mailto:frong0215@gmail.com)).

## I. INTRODUCTION

IN Korea, after the successful construction of Yongsoo OWC, which is a bottom fixed type installed on the west coast of Jeju Island and the capacity of which is a 500 kW, a new research project for the development of the breakwater integrated OWC has been carried out since 2016 with the support of Korean government. The purpose of the project is to develop a small OWC system which can be applied to the existing small breakwater in the remote island. In the process of evaluating the performance of the OWC chamber and developing the efficient design while carrying out the research project, KRISO (Korea Research Institute of Ships and Ocean engineering) has used a variety of methods including the model scale experiment, the potential flow based numerical analysis, and the CFD (Computational Fluid Dynamics) analysis.

A parametric study for choosing the concept of the OWC chamber applicable to the breakwater was done by using a frequency domain potential flow analysis which is based on a high-order boundary element method in addition to a wave flume model test. The sloped OWC chamber having a slope of 1/1.5, which is the same as the slope of the conventional breakwater in Korea, showed a good performance as well as good constructability in connection with existing breakwaters [1].

The detail design parameters of the sloped OWC chamber were studied by using a time domain potential flow analysis. Various size of the chamber length and skirt height was considered in the time domain simulation. The performance on irregular waves for various sea states was evaluated based on the regular wave simulations [2].

The experimental results from the wave flume model tests which are presented in [1] was validated by comparing it with a 2-dimensional CFD analysis. 2-dimensional wave flume simulations using the CFD for the sloped OWC chamber were performed to compare the relative wave height formed in the chamber for various incident wave conditions and showed good agreement with each other. In order to consider the effect of the PTO(Power Take-Off) of the OWC, the orifice was adopted into the 2-dimensional CFD analysis, and the performance characteristics was discussed [3, 4].

To avoid overestimating the primary energy conversion performance for the OWC, the standing waves inevitably generated by the wall effect when an OWC is installed in a 2-dimensional wave flume should be excluded. A model test for the 3-dimensional OWC model was done at a wave basin located in KRISO. The scaled OWC chamber modelled with a 1/4 of the scaling ratio and equipped the orifice to consider the PTO effect was faced regular waves generated in the basin with various periods. The relative wave height formed in the chamber, the differential pressure between before and after the orifice, and the airflow speed through the orifice were measured during the tests and compared with the CFD results obtained from the 3-dimensional simulations modelled on the same circumstances as that of the experiment. The 3-dimensional results of the experiment and CFD were validated by comparison with each other, and the performance of the sloped OWC was quantitatively evaluated [5].

Studies that we have done so far assumed that the OWC chamber is in a stand-alone state, not connected to a breakwater. In addition, there have been several literatures evaluating the performance of OWC integrated into breakwaters, but those have not been able to model the effect of wave dissipation by the realistic breakwater [6, 7]. Recalling the purpose of the research project, it is necessary to evaluate the performance of the OWC chamber in connection with breakwaters. The sloped OWC chamber is connected to the existing breakwaters, so there are tetrapods for wave dissipation around the chamber, and the breakwater foundation is located in the back of the chamber. The incident waves reflected and scattered from the tetrapods and the breakwater foundation can be disturbed, which may also change the performance of the chamber.

By using the CFD analysis method, the effect of the presence of the breakwater on the performance of the OWC chamber has been studied, even though unrealistic modelling was assumed where full reflection occurs by the breakwater foundation. The results showed that the standing waves created by the breakwater foundation in front of the OWC chamber can affect the performance of the chamber. Specifically, the performance was improved in a short wavelength region based on a specific incident wave period, and on the contrary, the performance was reduced in a long wavelength region. From the results, it can be predicted that when the tetrapods which is to dissipate the wave energy is modelled as the actual breakwater, the reflection wave is reduced and the creation of the standing wave is weakened, so that the performance improvement or the performance reduction effect depending on the incident wave periods can be weakened [8].

In order to assess the prediction, that is, to assess the extent of the effect on the chamber performance of the presence of the breakwater, it was necessary to experimentally evaluate the performance of the

breakwater integrated OWC chamber. In this study, experimental results for the performance evaluation of the OWC chamber without and with the breakwater integration were presented with the description of the method for the experimental modelling. The rest of the paper is organized as follows; First, the OWC chamber and the breakwater model is defined, followed by the

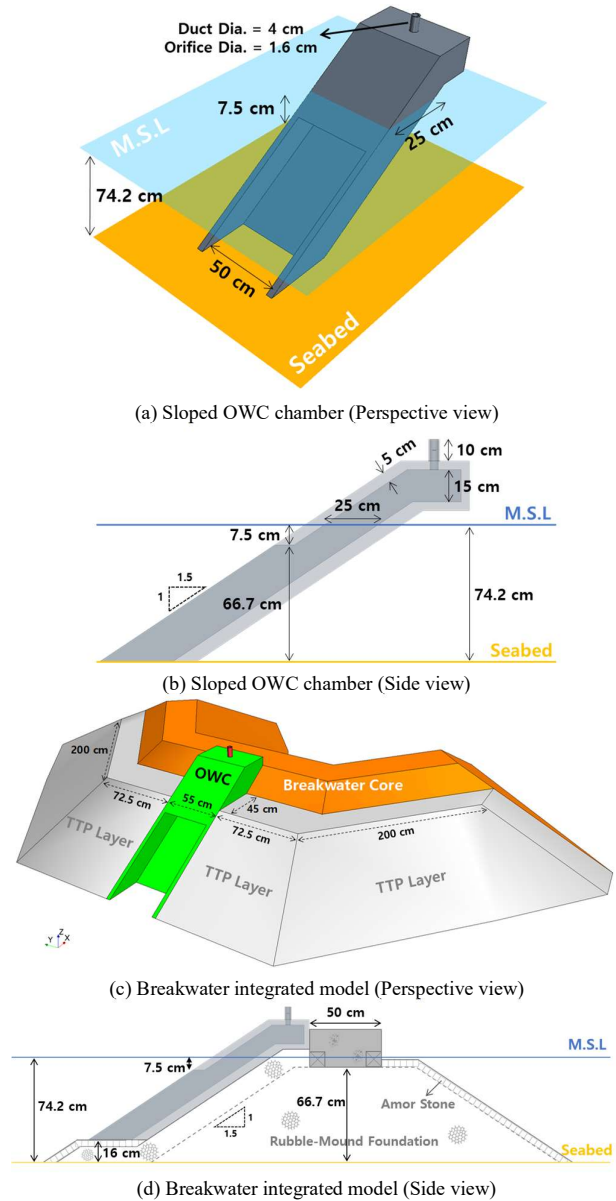


Fig. 1. Description of sloped OWC chamber and breakwater integrated model.

description of the experimental methods. Next, the results and discussions are presented, and finally, concluding remarks are provided.

## II. PROBLEM DESCRIPTION

The sloped OWC chamber designed through the previous studied was adopted as the experimental model, and the chamber was connected to the breakwater which was modelled by idealizing Mungni Port in Chuja Island

where the demonstration test for the developed OWC system is planned [8]. Fig 1 shows the geometry of the adopted OWC chamber as well as the breakwater integrated model with principal dimensions in model scale. The chamber, the inner length and width of which are 25 cm and 50cm, respectively and the skirt depth of which is 7.5 cm and was installed on the bottom of a wave basin of 0.742 meters depth. The duct, the diameter of which is 4 cm, connecting the inside of the chamber and atmosphere is on the top of the chamber, and it was equipped the orifice to model the turbine effects with 1.6 cm of a diameter. The OWC chamber will be placed where the TTP (Tetrapod) is removed as described at Fig. 1 (c). The TTPs were accumulated as a double layer along the sloped surface of the breakwater.

### III. EXPERIMENTAL METHODS

The experimental was carried out at a shallow water wave basin owned by Waterfront and Coastal Research

Center (WCRC) of Catholic Kwandong University (CKU) in Korea, the length and width of which are 35 m and 30m, respectively. The depth of the basin can be adjustable up to 1 m, and it is equipped with a piston-type wave generator and revetments for wave absorption.

The experimental model was scaled based on Froude scaling with a ratio of 1/20. Table 1 compares the principal dimensions of the prototype and the

TABLE I  
PRINCIPAL DIMENSIONS OF EXPERIMENTAL MODEL

| Dimensions of OWC         | Scale     | 1/20       |
|---------------------------|-----------|------------|
| Items                     | Prototype | Exp. Model |
| Water Depth               | 14.84 m   | 74.2 cm    |
| Chamber Length            | 5 m       | 25 cm      |
| Chamber Width             | 10 m      | 50 cm      |
| Skirt Depth               | 1.5 m     | 7.5 cm     |
| Skirt Thickness           | 1 m       | 5 cm       |
| Duct Diameter             | 0.8 m     | 4 cm       |
| Duct Height               | 2 m       | 10 cm      |
| Orifice Diameter          | -         | 1.6 cm     |
| TTP Weight                | 28.75 ton | 3.59 kg    |
| TTP Diameter              | 3.82 m    | 19.1 cm    |
| TTP Height                | 3.55 m    | 17.75 cm   |
| Double-Layered TTP Height | 4.73 m    | 23.65 cm   |

experimental model, and Fig. 2 shows the experimental model for the OWC chamber, TTP, and the integrated model without being filled with water in the basin.

To evaluate the performance of the primary energy conversion of the OWC, the differential pressure between before and after the orifice and the airflow speed were measured in addition to the water surface elevation inside the chamber. The water surface elevation was measured using a calibrated wave gauge installed along the sloped surface at a centre position in the chamber.



(a) OWC chamber model



(b) Tetrapod model



(c) Integrated model

Fig. 2. Installed experimental model.

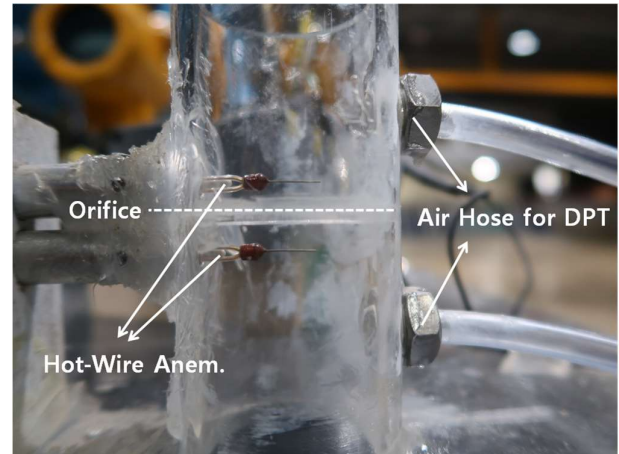


Fig. 3. Installed differential pressure transmitter (DPT) and hot-wire anemometer.

The differential pressure between before and after the orifice was obtained by using a differential pressure transmitter, APR-2000ALW manufactured by Aplisens. It was set to measure the differential pressure in a range of  $\pm 1,500$  Pa with up to 16 ms intervals, and the measurement error can be up to  $\pm 0.075\%$  for the



maximum value. Two air hoses adopted to collect the pressure from above the orifice and below the orifice, respectively, to the transmitter was attached to each points, which were 2.5cm above and below the duct centre height where the orifice was located. The airflow speed through the orifice was measured by using two hot-wire anemometer, model No. 8465 manufactured by TSI, which can measure airflow speeds in a range of 0 to 50 m/s at intervals of up to 20 ms with the measurement error of up to  $\pm 2.5\%$  for the maximum value. The hot-wire anemometers were installed at two point, which were 0.7 cm above and below the orifice. Fig. 3 shows the installed instruments for measuring the differential pressure and the airflow speed. Measured signals were obtained at a data acquisition device with a sampling frequency of 50 Hz, and were analysed to get the mean amplitude and mean height from the time series interval in which the signal is periodically maintained by applying a zero-up crossing method.

Table 2 shows the wave characteristics applied to the experiment. Note that the subscripts M and R denote the real scale and the model scale, respectively, as well as T,  $\lambda$ , and H represent the wave period, the wavelength, and the wave height for the incident waves, respectively. Three sets of the wave slope level for regular waves was considered. The low, medium, and high correspond to 0.007, 0.012, and 0.02 of the wave slope, which is defined

TABLE II  
REGULAR WAVE CHARACTERISTICS APPLIED TO EXPERIMENT

| $T_M$<br>(s) | $\lambda_M$<br>(m) | $T_R$<br>(s) | $\lambda_R$<br>(m) | H (m)                          |                                   |                                |
|--------------|--------------------|--------------|--------------------|--------------------------------|-----------------------------------|--------------------------------|
|              |                    |              |                    | Low,<br>$H/\lambda$<br>= 0.007 | Medium,<br>$H/\lambda$<br>= 0.012 | High,<br>$H/\lambda$<br>= 0.02 |
| 0.80         | 1.00               | 3.58         | 19.98              | 0.007                          | 0.012                             | 0.020                          |
| 1.00         | 1.55               | 4.47         | 31.06              | 0.011                          | 0.019                             | 0.031                          |
| 1.20         | 2.19               | 5.37         | 43.71              | 0.015                          | 0.026                             | 0.044                          |
| 1.40         | 2.84               | 6.26         | 56.77              | 0.020                          | 0.034                             | 0.057                          |
| 1.60         | 3.48               | 7.16         | 69.65              | 0.024                          | 0.042                             | 0.070                          |
| 1.90         | 4.42               | 8.50         | 88.35              | 0.029                          | 0.049                             | 0.082                          |
| 2.20         | 5.32               | 9.84         | 106.45             | 0.037                          | 0.064                             | 0.106                          |

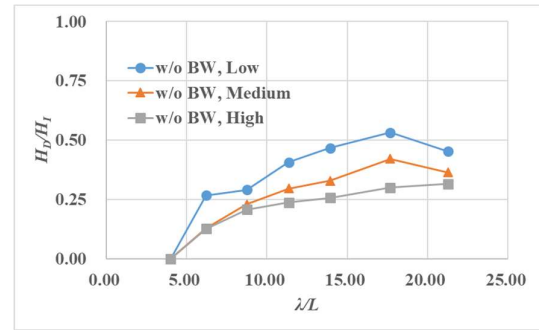
as the wave height divided by the wavelength, respectively. The wave period for the each set was varied from 0.8 sec to 2.2 sec in model scale.

#### IV. RESULTS AND DISCUSSION

Results of regular wave tests for various wave slopes, listed at Table 2, without the integration of the breakwater, that is the OWC chamber is installed alone, were summarized in Fig. 4. The relative wave height, which is defined as a ratio of the induced wave height in the chamber ( $H_D$ ) to the incident wave height ( $H_I$ ), was shown at Fig. 4 (a). The differential pressure between before and after the orifice during the pressurization and de-pressurization plotted at Fig. 4 (b) and (c), respectively. Note that  $\rho$  is a water density,  $g$  is a

gravitational acceleration, and  $A_I$  is the incident wave amplitude. In addition, the airflow speed through the orifice during the outflow and inflow depicted at Fig. 4 (d) and (e), respectively. Note that  $\omega$  is an incident wave frequency in rad/sec. The variable indicated at the horizontal axis in Fig. 4,  $\lambda/L$ , is a non-dimensionalized parameter, for which  $\lambda$  is an incident wavelength and  $L$  is the chamber length defined as the horizontal distance between the skirt and the rear wall inside the chamber. From the results, the differential pressure was independent of incident wave slope, whereas the relative wave height and the airflow speed were dependent. It can be seen that the relative wave height and the non-dimensionalized airflow speed are lowered as the wave slope becomes larger. Predicted from those dependency, the efficiency of the primary energy conversion, which is defined as the ratio of the pneumatic energy proportional to the product of the differential pressure and the airflow rate to the incident wave energy proportional to the square of the incident wave height [9], can be evaluated higher as the wave slope of the incident wave is lower.

Fig. 5 shows the results for evaluating the performance effects with and without the breakwater for the OWC chamber at the medium level of the wave slope listed at Table 2. It can be seen that the pneumatic energy of the OWC chamber integrated into the breakwater is lower than that of the isolated chamber except the point where the non-dimensionalized wavelength is higher than 20. This is different from the result of CFD modelling in the previous research [8] that the breakwater was assumed as the rigid wall. It is because the standing wave is not formed as the TTPs effectively dissipated the incident wave in the relatively short wavelength region. On the other hands, at a point where the non-dimensionalized wavelength is higher than 20, a relatively long wave is not sufficiently dissipated by the TTPs and a standing wave that improves the performance as shown in the previous results presented in [8] is created due to a large amount of reflected waves.



(a) Relative wave height

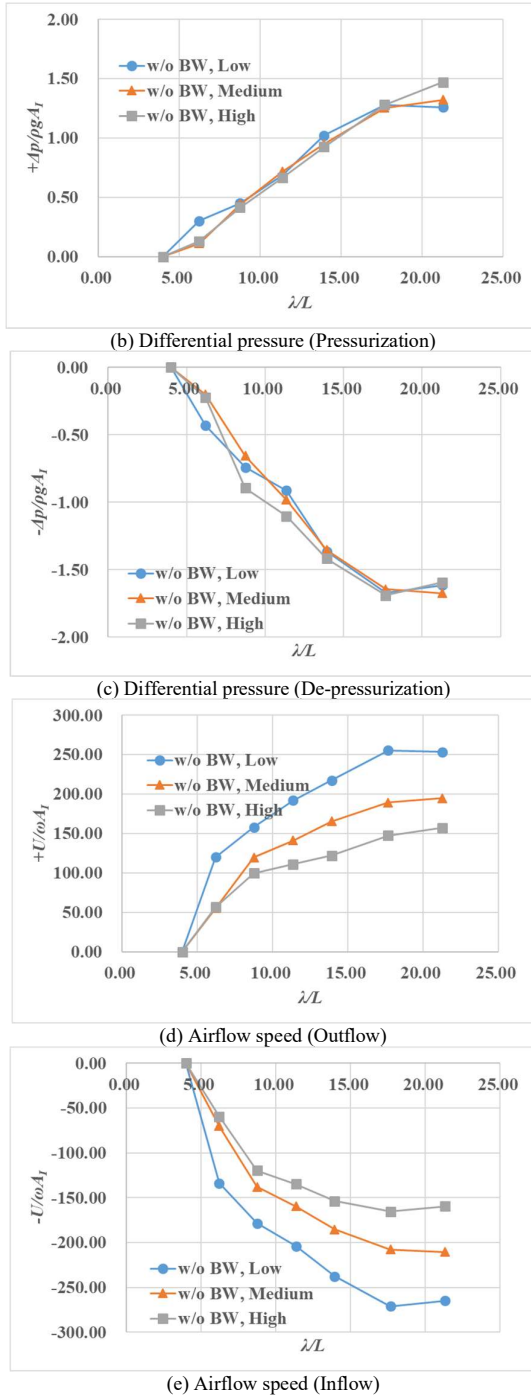


Fig. 4. Measurement results without breakwater integration for various wave slope conditions .

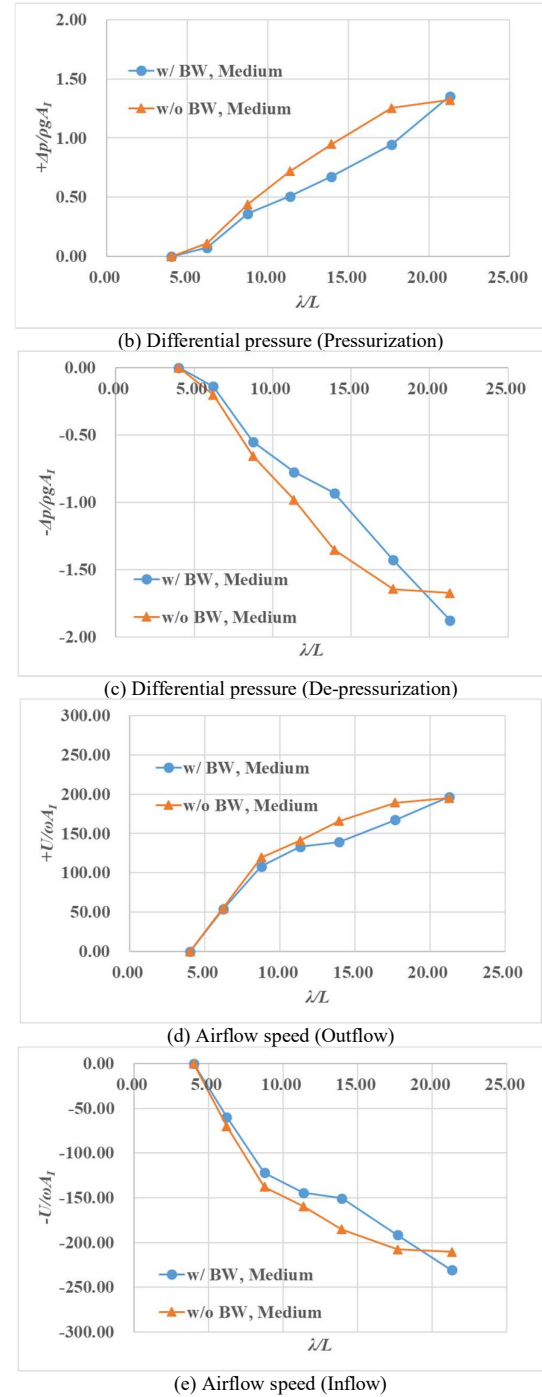


Fig. 5. Comparison between with and without breakwater integration for medium slope condition.

## V. CONCLUDING REMARKS

In this study, experimental results to evaluate the performance of the sloped OWC chamber for various wave conditions with and without the breakwater integration were presented. The dependency on the incident wave slope of the performance for the OWC chamber was studied, specifically, the higher the wave slope, the lower the relative wave height in the chamber and the non-dimensionalized airflow speed. The effect of breakwaters on the OWC performance was discussed by

comparing the measurement results with and without the breakwater integration. In a relatively short wave region where the non-dimensionalized wavelength is less than 20, it seems that the incident waves were effectively dissipated by the TTPs, and the performance of OWC was reduced by the breakwater effect. In a relatively long wave region where the non-dimensionalized wavelength is higher than 20, it seems that the incident wave is not sufficiently dissipated by the TTPs and the reflected waves are generated, resulting in the creation of the standing waves that improve the performance of the OWC chamber.

In the future, the CFD analysis considering the effect of the wave dissipation by the TTPs will be done to investigate the cause of the performance change for the OWC chamber by the presence of the breakwater.

#### REFERENCES

- [1] S. Park, B. W. Nam, K-H. Kim, K. Hong, "Parametric study on oscillating water column wave energy converter applicable to breakwater," *Journal of Advanced Research in Ocean Engineering*, vol. 4, no. 2, pp. 66-77, 2018. DOI: <http://dx.doi.org/10.5574/JAROE.2018.4.2.066>, [Online].
- [2] J-S. Kim, B. Nam, K-H. Kim, K. Hong, "Cross-sectional shape design of OWC chamber of wave energy converter applicable to breakwater," in *8th East Asian Workshop for Marine Environment and Energy*, Jeju, Korea, 2017, pp. 163-169.
- [3] S. Park, K-H. Kim, B-W. Nam, J-S. Kim, K. Hong, "Numerical study on performance analysis for OWC WEC applicable to breakwater," in *4th Asian Wave and Tidal Energy Conference*, Taipei, Taiwan, 2018.
- [4] S. Park, K-H. Kim, B. W. Nam, J-S. Kim, K. Hong, "A study on the performance evaluation of the OWC WEC applicable to breakwaters using CFD," *Journal of Korean Soc. Mar. Environ. Energy*, vol. 21, no. 4, pp. 317-327, 2018. DOI: <https://doi.org/10.7846/JKOSMEE.2018.21.4.317>, [Online]
- [5] S. Park, K-H. Kim, B-W. Nam, J-S. Kim, K. Hong, "Experimental and numerical analysis of performance of oscillating water column wave energy converter applicable to breakwaters," in *38th International Conference on Ocean, Offshore, and Arctic Engineering*, Glasgow, Scotland, 2019, OMAE2019-96500 (To be published on June, 2019).
- [6] Z. Liu, H. Shi, B-S. Hyun, "Practical design and investigation of the breakwater OWC facility in China," in *8th European Wave and Tidal Energy Conference*, Uppsala, Sweden, 2009, pp. 304-308.
- [7] D. Howe and J-R. Nader, "OWC WEC integrated within a breakwater versus isolated: Experimental and numerical theoretical study," *International Journal of Marine Energy*, vol 20, pp. 165-182, 2017. DOI: <https://doi.org/10.1016/j.ijome.2017.07.008>
- [8] S. Park, K-H. Kim, B.W. Nam, J-S. Kim, K. Hong, "A study on effects of breakwater on performance of OWC," in *13th Pacific-Asia Offshore Mechanics Symposium*, Jeju, Korea, 2018, pp. 351-356.
- [9] I. López, G. Iglesias, "Efficiency of OWC wave energy converters: a virtual laboratory," *Journal of Applied Ocean Research*, vol. 44, pp. 63-70, 2014. DOI: <https://doi.org/10.1016/j.apor.2013.11.001>